A NEW DESIGN OF ROBUST DIGITAL CONTROLLER FOR DC-DC CONVERTERS

Kohji Higuchi * **Kazushi Nakano** *
Tatsuyoshi Kajikawa * **Eiji Takegami** **
Satoshi Tomioka ** **Kazushi Watanabe** **

* *Dept. of Electronic Engineering, The University of Electro-Communications, 1-5-1 Chofu-ga-oka, Chofu, Tokyo 182-8585, Japan*
** *DENSEI-LAMBDA K.K., 2701 Togawa, Settaya, Nagaoka 940-1195, Japan*

Abstract: Robust DC-DC converters which can cover extensive load changes and also input voltage changes are needed. In this paper, we propose a new method for designing good approximate 2-degree-of freedom (2DOF) digital controller which makes the control bandwidth wider, and at the same time makes a variation of the output voltage very small at sudden changes of resistive load. The proposed approximate 2DOF digital controller is actually implemented on a DSP and is connected to a DC-DC converter. Experimental studies demonstrate that this type of digital controller can satisfy given specifications.

Keywords: DC-DC converter, Digital Control, Approximate 2-degree-of-freedom system, Robust control

1. INTRODUCTION

In many applications of DC-DC converters, loads cannot be specified in advance, i.e., their amplitudes are suddenly changed from the zero to the maximum rating. Generally, design conditions are changed for each load and then each controller has to be re-designed. Then, a so-called robust DC-DC converter which can cover such extensive load changes and also input voltage changes with one controller is needed. Analog control IC is used usually for the controller of DC-DC converters. Simple integral control etc. are performed with the analog control IC. Moreover, the application of the digital controller to DC-DC converters designed by the PID or root locus method etc. has been considered recently (Guo. L, 2003, Guo. H, 2003). However it is difficult to retain sufficient robustness of DC-DC converters by these techniques.

The authors proposed the method of designing an approximate 2-degree-of-freedom (2DOF) robust controller of DC-AC converters (Higuchi, *et al.*, 2002, 2003). For applying this approximate 2DOF controller to DC-DC converters, it is necessary to improve the degree of approximation for better robustness. In this paper, we propose a new method for designing good approximate 2DOF digital controller which makes the control bandwidth wider, and at the same time makes a variation of the output voltage very small at sudden changes of resistive load. We also show the controller parameter design procedure which performs good approximation. This type of good approximate 2DOF controller is constituted as follows : First, a model matching system with a specified rising time in startup transient response is constituted by using the voltage and the current feedbacks. The current sensor is generally expen-

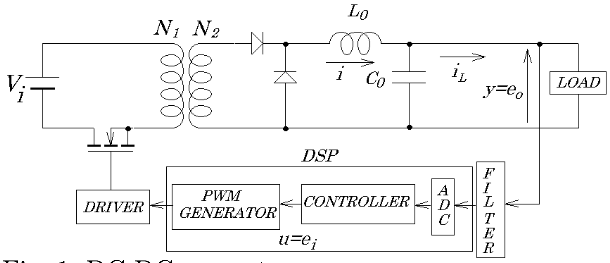

Fig. 1. DC-DC converter

sive and noisy. In order to avoid use of the current sensor, the current feedback is changed by using a dynamic compensator into the output feedback and control input feedback equivalently. Secondly, a first order approximate model of this model matching system is derived. And inverse system of this first order approximate model and a filter for realizing the inverse system are combined with the model matching system. Finally, an equivalent conversion of the portion of the controller is carried out, and a realizable approximate 2DOF controller is obtained. This digital controller is actually realized by using a DSP. Some simulations and experiments show that the proposed high-order approximate 2DOF digital controller can satisfy given specifications.

2. DC-DC CONVERTER

The DC-DC converter as shown in **Fig.1** has been manufactured. In order to realize the approximate 2DOF digital controller which satisfies given specifications, we use $TITMS320LF$ 2401 as DSP. This DSP has a built-in AD converter and a PWM switching signal generating part. The triangular wave carrier is adopted as a PWM switching signal generating part. The switching frequency is set at 300[KHz] and the peak-to-peak amplitude C_m is 66[V]. The LC circuit is a filter for removing carrier and switching noises. L_0 is 1.4[μH], and C_0 is 308[μF]. If the frequency of control input u is smaller enough than that of the carrier, the state equation of the DC-DC converter at resistive load in Fig.1 except DSP can be expressed from the state equalizing method (Fukuda and Nakaoka, 1993) as follows:

$$\begin{cases} \dot{x} = A_c x + B_c u \\ y = Cx \end{cases} \qquad (1)$$

where

$$x = \begin{bmatrix} e_o \\ i \end{bmatrix} \quad A_c = \begin{bmatrix} -\dfrac{1}{C_0 R_L} & \dfrac{1}{C_0} \\ -\dfrac{1}{L_0} & -\dfrac{R_0}{L_0} \end{bmatrix} \quad B_c = \begin{bmatrix} 0 \\ \dfrac{K_p}{L_0} \end{bmatrix}$$

$$C = \begin{bmatrix} 1 & 0 \end{bmatrix} \quad u = e_i \quad y = e_0 \quad K_p = -\frac{V_i N_2}{C_m N_1}$$

When realizing a digital controller by a DSP, a delay time exists between the start point of sampling

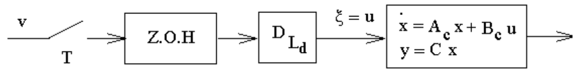

Fig. 2. Controlled object with input dead time $L_d(\le T)$

operation and the output point of control input due to the input computing time and AD/DA conversion times. This delay time is considered to be equivalent to the input dead time which exists in the controlled object as shown in **Fig.2**.

Then the state equation of the system of Fig.2 is expressed as follows:

$$\begin{cases} x_{dw}(k+1) = A_{dw} x_{dw}(k) + B_{dw} v(k) \\ y(k) = C_{dw} x_{dw}(k) \end{cases} \qquad (2)$$

where

$$x_{dw}(k) = \begin{bmatrix} x_d(k) \\ \xi_2(k) \end{bmatrix} \quad x_d(k) = \begin{bmatrix} x(k) \\ \xi_1(k) \end{bmatrix}$$

$$A_{dw} = \begin{bmatrix} A_d & B_d \\ 0 & 0 \end{bmatrix} \qquad B_{dw}(k) = \begin{bmatrix} 0 \\ 1 \end{bmatrix}$$

$$A_d = \begin{bmatrix} e^{A_c T} & e^{A_c (T-L_d)} \displaystyle\int_0^{L_d} e^{A_c \tau} B_c d\tau \\ 0 & 0 \end{bmatrix}$$

$$B_d = \begin{bmatrix} \displaystyle\int_0^{T-L_d} e^{A_c \tau} B_c d\tau \\ 1 \end{bmatrix}$$

$$C_{dw} = \begin{bmatrix} C_d & 0 \end{bmatrix} \quad C_d = \begin{bmatrix} C & 0 \end{bmatrix} \quad \xi_1(k) = u(k)$$

In practical use of DC-DC converter, the characteristics of a startup transient response and a dynamic load response are important. The DC-DC converter with the following specifications (1)-(6) is designed and manufactured by constituting digital controller to DC-DC switching part.

(1) Input voltage V_i is 48[V] and output voltage e_o is 3.3[V].
(2) Startup transient reponses are almost the same at resistive load and parallel load of resistance and capacity, where $0.165 \le R_L < \infty[\Omega]$, $0 \le C_L \le 200[\mu$F].
(3) The rising time in startup transient reponse is smaller than 100[μs].
(4) Against all the loads of spec.2, an over-shoot is not allowable in startup transient response.
(5) The dynamic load response is smaller than 50[mV] against 10[A] change of load current.
(6) The specs. (2),(3),(4) and (5) are satisfied also to change of input voltage of $\pm 20\%$.

The load changes for the controlled object and the input voltage change are considered as parameter changes in eq.(2). Such parameter changes can be

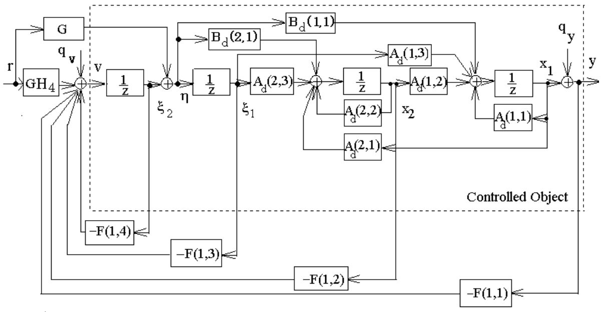

Fig. 3. Equivalent disturbances due to load variations (parameter variations) and model matching system with state feedback

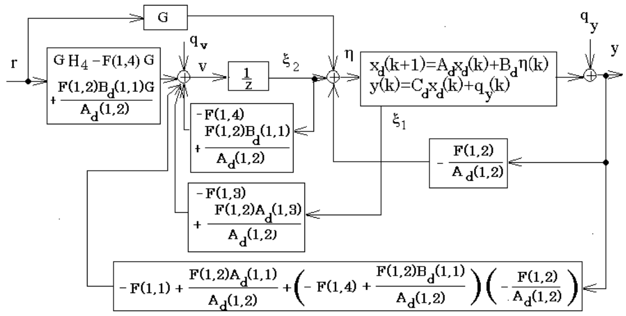

Fig. 4. Model matching system using only voltage (output) feedback

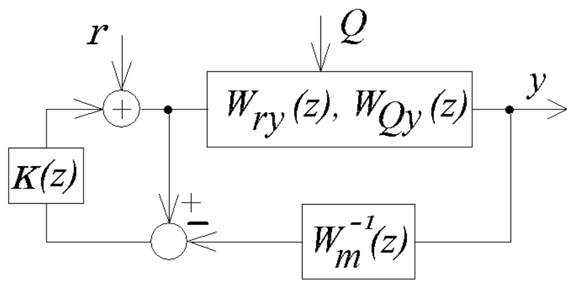

Fig. 5. System reconstituted with an inverse system and a filter

transformed to equivalent disturbances q_v and q_y as shown in **Fig.3** even in discrete-time systems. Moreover, if the saturation in the input arises or the input frequency is not so small as the carrier frequency, the controlled object will be regarded as a class of nonlinear systems. Such characteristics changes can be also transformed to equivalent disturbances as shown in Fig.3. Therefore, what is necessary is just to constitute the control systems whose pulse transfer functions from equivalent disturbances q_v and q_y to the output y become as small as possible in their amplitudes, in order to robustize or suppress the influence of these parameter changes, i.e., load changes, and input voltage change. In the next section, an easily designing method which makes it possible to suppress the influence of such disturbances with the target characteristics held will be presented.

3. DESIGN OF GOOD APPROXIMATE 2DOF DIGITAL INTEGRAL-TYPE CONTROL SYSTEM

First, the transfer function between the reference input r and the output y is specified as follows: $W_{ry} =$

$$\frac{(1+H_1)(1+H_2)(1+H_3)(z-n_1)(z-n_2)(z+H_4)}{(1-n_1)(1-n_2)(z+H_1)(z+H_2)(z+H_3)(z+H_4)} \tag{3}$$

where, n_1 and n_2 are the zeros for discrete-time control object (2). It shall be specified that the relation of H_1 and H_2, H_3 becomes $|H_1| \gg |H_2|$ and $|H_3|$. Then $W_{ry}(z)$ can be approximated in the following manner:

$$W_{ry}(z) \approx W_m(z) = \frac{1+H_1}{z+H_1} \tag{4}$$

This target characteristic $W_{ry}(z) \approx W_m(z)$ is specified to satisfy the specs.(3) and (4).

Applying a state feedback

$$v = -Fx^* + GH_4 r \tag{5}$$

$$x^* = [y \quad x_2 \quad \xi_1 \quad \xi_2]^T$$

and feedforward

$$\xi_1(k+1) = Gr \tag{6}$$

to the discrete-time controlled object as shown in Fig.3, we decide $F = [F(1,1)\ F(1,2)\ F(1,3)\ F(1,4)]$ and G so that $W_{ry}(z)$ becomes eq.(3). Th current feedback is used in Fig.3. This is transformed to voltage and control input feedbacks, without changing the pulse transfer function between $r-y$ by an equivalent conversion. The following relation is obtained from Fig.3:

$$\begin{aligned} -F(1,2)x_2(k) = &-\frac{F(1,2)}{A_d(1,2)}(x_1(k+1) \\ &-A_d(1,1)x_1(k) - A_d(1,3)\xi_1 - B_d(1,1)\eta) \end{aligned} \tag{7}$$

If the current feedback is transformed equivalently using the right-hand side of this equation, the control system with only voltage feedback as shown in **Fig.4** will be obtained. The transfer function $W_{Qy}(z)$ between this equivalent disturbance $Q = [q_v \quad q_y]^T$ and y of the system in Fig.4 is desfined as

$$W_{Qy}(z) = \left[\, W_{q_v y}(z)\ W_{q_y y}(z) \,\right] \tag{8}$$

The system added the inverse system and filter to the system in Fig.4 is constituted as shown in **Fig.5**. In Fig.5, the transfer function $F(z)$ becomes

$$F(z) = \frac{k_z}{z-1+k_z} \tag{9}$$

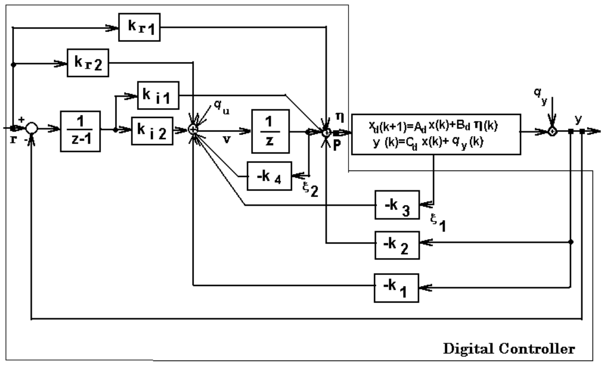

Fig. 6. Approximate 2DOF digital integral-type control system

The transfer functions between $r-y$ and $Q-y$ of the system in Fig.5 are given by

$$y = \frac{(1+H_1)}{(z+H_1)}\frac{z-1+k_z}{z-1+k_zW_s(z)}W_s(z)r \quad (10)$$

$$y = \frac{z-1}{z-1+k_z}\frac{z-1+k_z}{z-1+k_zW_s(z)}W_{Qy}(z)Q \quad (11)$$

where

$$W_s(z) = \frac{(1+H_2)(1+H_3)(z-n_1)(z-n_2)}{(z+H_2)(z+H_3)(1-n_1)(1-n_2)} \quad (12)$$

Here, if $W_s(z) \approx 1$, then eqs.(10) and (11) become, respectively,

$$y \approx \frac{1+H_1}{z+H_1}r \quad (13)$$

$$y \approx \frac{z-1}{z-1+k_z}W_{Qy}(z)Q \quad (14)$$

From eqs.(13) and (14), it turns out that the characteristics from r to y can be specified with H_1, and the characteristics from Q to y can be independently specified with k_z. That is, the system in Fig.5 is an approximate 2DOF system, and its sensitivity against disturbances, i.e., load change becomes lower with the increase of k_z.

If an equivalent conversion of the controller in Fig.5 is carried out, the approximate 2DOF digital integral-type control systems will be obtained as shown in **Fig.6**. In Fig.6, the parameters of the controller are as follows:

$$\begin{aligned}
k_1 &= F(1,1+F(1,2)FF(1,1)+((-F(1,4)\\
&\quad -F(1,2)FF(1,4))(-F(1,2)/FF(1,2)))\\
&\quad +(GH4+GF_z)(k_z/(1+H2))\\
k_2 &= F(1,2)/FF(1,2)+G(k_z/(1+H2))\\
k_3 &= F(1,3)+F(1,2)(FF(1,3)) \quad k_4 = -F_z\\
k_{i1} &= Gk_z \quad k_{i2} = (GH4+GFz)k_z\\
k_{r1} &= G \quad k_{r2} = GH4+GF_z \qquad (15)
\end{aligned}$$

where

$$\begin{aligned}
FF(1,1) &= -A_d(1,1)/A_d(1,2)\\
FF(1,2) &= A_d(1,2)\\
FF(1,3) &= -A_d(1,3)/A_d(1,2)\\
FF(1,4) &= -B_d(1,1)/A_d(1,2)\\
F_z &= -F(1,4)-F(1,2)FF(1,4)
\end{aligned}$$

Now, for good approximation, i.e., for letting eqs.(10) and (11) approach further to the right-hand sides of eqs.(13) and (14) respectively, what is necessary is just to set up so that $W_s(z)$ may approach further to 1 in the large frequency range. What is necessary is just to suitably determine H_2 and H_3, after determining H_1 and H_4 so that the target characteristics may be satisfied. In other words, what is necessary is setting up H_2 and H_3 as small as possible. For good approximation, the design procedure of the parameters of the controller is shown as follows:

(1) H_1 is set up so that the specified rising time is satisfied.
(2) H_4 is set up as

$$|H_4| \approx 0.5|H_1| \quad (16)$$

(3) The roots of the following equation:

$$z-1+k_zW_s(z) = 0 \quad (17)$$

are set up as

$$p_1 \approx -0.5H_1+0.5H_1i \quad p_2 \approx -0.5H_1-0.5H_1i$$
$$p_3 \approx -0.5H_1 \quad (18)$$

(4) k_z of eq.(17) are set up as

$$k_z \approx 0.5 \quad (19)$$

(5) Determin H_2 and H_3 so that the roots of eq.(17) become equal to p_1, p_2 and p_3.
(6) Determine the parameters of the controller from eq.(15).
(7) Check whether all the specifications are satisfied by simulation.
(8) When not satisfying the specification, (4) is changed a little and the next (5) are repeated.
(9) Furthermore when not satisfying the specification, (3) is changed a little and the next (4) are repeated.

4. EXPERIMENTAL STUDIES

The sampling period T are set as $3.3[\mu s]$ and the input dead time L_d is about $0.999T[\mu s]$. We will design a control system so that all the specifications are satisfied. First of all, in order to satisfy the specification on the rising time in startup transient reponse, from design procedures (1) and (2), H_1, and H_4 are set as

$$H_1 = -0.89 \quad H_4 = -0.3 \tag{20}$$

In order to increase the degree of the approximation in eqs.(13) and (14) over the large frequency range, what is necessary is just to make the absolute value of the real part of the roots of eq.(17) as small as possible. Eq.(17) is changed equivalently to

$$\begin{aligned}\Delta(z) = &(1-n_1)(1-n_2)(z-1)(z+H_2)(z+H_3)\\ &+ k_z(1+H_2)(1+H_3)(z-n_1)(z-n_2)\end{aligned} \tag{21}$$

Substituting

$$H_2 = x + yi \quad H_3 = x - yi \tag{22}$$

into eq.(21), we get

$$\begin{aligned}&(\ k_z x^2 + (2k_z - 2n_2 + 2n_1 n_2 - 2n_1 + 2)x\\ &+ k_z y^2 + (-1 + n_2 + k_z - n_1 n_2 + n_1))/(1 - n_2 - n_1\\ &+ n_1 n_2) = -p_1 - p_3 - p_2\end{aligned} \tag{23}$$

$$\begin{aligned}&(\ (-k_z n_1 + n_1 n_2 - n_2 + 1 - n_1 - k_z n_2)x^2\\ &+ (2n_2 + 2n_1 - 2k_z n_2 - 2n_1 n_2 - 2k_z n_1 - 2)x\\ &+ (-k_z n_1 + n_1 n_2 - n_2 + 1 - n_1 - k_z n_2)y^2\\ &- k_z n_2 - k_z n_1)/(1 - n_2 - n_1 + n_1 n_2)\\ &= p_1 p_3 + p_1 p_2 + p_2 p_3\end{aligned} \tag{24}$$

$$\begin{aligned}&(\ (-1 + n_2 + k_z n_1 n_2 - n_1 n_2 + n_1)x^2\\ &+ 2k_z n_1 n_2 x + (-1 + n_2 + k_z n_1 n_2\\ &- n_1 n_2 + n_1)y^2 + k_z n_1 n_2)(1 - n_2 - n_1\\ &+ n_1 n_2) = -p_1 p_2 p_3\end{aligned} \tag{25}$$

These are circle equations when fixing k_z. From procedures (3) and (4), setting as

$$\begin{aligned}&p1 = 0.35 + 0.5i \quad p2 = 0.35 - 0.5i \quad p3 = 0.5\\ &k_z = 0.3 \quad n_1 = -0.97351 \quad n_2 = -.97731e6\end{aligned} \tag{26}$$

and substituting these into eqs.(23),(24) and (25), we get

$$2x + 0.0000016x^2 + 0.0000016y^2 + 0.2 = 0 \tag{27}$$
$$-1.696x + 1.152x^2 + 1.152y^2 - 0.570 = 0 \tag{28}$$
$$0.296x - 0.852x^2 - 0.852y^2 + 0.334 = 0 \tag{29}$$

These circles are drawn in **Fig.7**. From the intersect point, we get

$$x = -0.1 \quad y = 0.6 \tag{30}$$

Then, from the procedure (6), the parameters of controller become

$$\begin{aligned}&k_1 = -332.223 \ \ k_2 = 260.57 \ \ k_3 = -0.51638\\ &k_4 = -0.51781 \ k_i = 7.0594 \ k_{iz} = -8.6321\end{aligned} \tag{31}$$

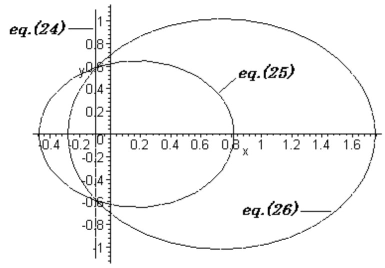

Fig. 7. Circles of eqs.(27),(28) and (29)

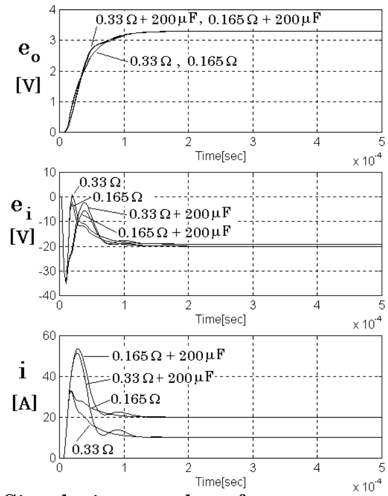

Fig. 8. Simulation results of startup responses at various loads

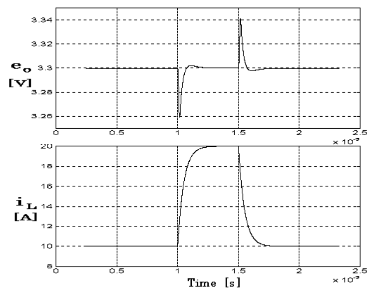

Fig. 9. Simulation result of dynamic load response at resistive load

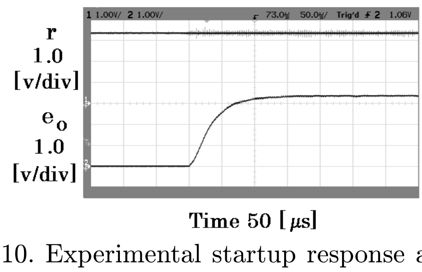

Fig. 10. Experimental startup response at $R_L = 0.33[\Omega]$

It must be better that k_{r1} and k_{r2} are set to 0, since the characteristics of the control system hardly changes in this case.

The simulation results of the startup responses are shown in **Fig.8**. From the output voltage $y = e_o$ in this figure, it turns out that the specifications are satisfied. It is checked that almost the same simulation results as Fig.8 are obtained when the

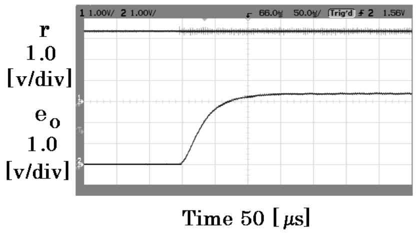

Fig. 11. Experimental startup response at $R_L = 0.165[\Omega]$

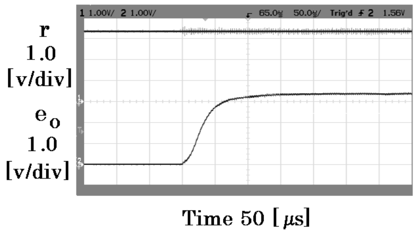

Fig. 12. Experimental startup response at parallel load of $R_L = 0.33[\Omega]$) and $C_L = 200[\mu\text{F}]$

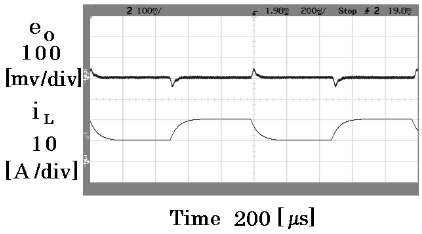

Fig. 13. Experimental dynamic load response at $R_L = 0.33 \leftrightarrow 0.165[\Omega]$

input voltage V_i is changed by $\pm 20\%$. The simulation result of the dynamic load responses is shown in **Fig.9**. Fig.9 is the result at resistive load and the value is changed as $R_L = 0.33 \leftrightarrow 0.165[\Omega]$. It is checked that almost the same simulation result as Fig.9 is obtained at parallel load of resistance ($R_L = 0.33 \leftrightarrow 0.165[\Omega]$) and capacity ($C_L = 200[\mu\text{F}]$). It turns out that all the specifications are satisfied.

Experimental results when realizing the digital controller with the parameters of eq.(31) by using the DSP, and connecting to the controlled object of eq.(1) are shown in **Figs.10-13**. Fig.10 and Fig.11 show startup responses at resisitive loads $R_L = 0.33[\Omega]$ and $R_L = 0.165[\Omega]$, respectively. Fig.12 shows a startup response at parallel load of resistance $R_L = 0.33[\Omega]$ and capacity $C_L = 200[\mu\text{F}]$. From $y = e_o$ in these figure, it turns out that almost the same exprimental results as the simulation ones in Fig.8 are obtained and the specifications are satisfied. It is checked that almost the same exprimental results as the simulation ones in Fig.8 are obtained at the parallel load of resistance $R_L = 0.165[\Omega]$ and capacity $C_L = 200[\mu\text{F}]$. It is checked that almost the same exprimental results as Fig.10 are obtained at resisitive load $R_L = 0.33[\Omega]$ when the input voltages are 58[V] and 38[V]. It turns out that the specifications are satisfied when the input voltage V_i is changed by $\pm 20\%$. Fig.13 shows a dynamic load response at resistive load and the value changed as $R_L = 0.33 \leftrightarrow 0.165[\Omega]$. It turns out tha almost the same exprimental results as the simulation results in Fig.9 are obtained. It is checked that almost the same exprimental results as Fig.13 are obtained at the parallel load of resistance ($R_L = 0.33 \leftrightarrow 0.165[\Omega]$) and capacity ($C_L = 200[\mu\text{F}]$). Although load current(i_L) changed suddenly from 20 [A] to 10 [A] or reverse, output voltage change is very small and is suppressed within about 50[mV]. It turns out that all the specification are satisfied.

5. CONCLUSION

In this paper, the concept for controller of DC-DC converter to attain the good robustness against an extensive load changes and input voltage change was given. The proposed digital controller was implemented on the DSP connecting to the controlled object. It was shown from some simulations and experiments that a sufficiently robust digital controller is realizable. The characteristics of the startup transient response and the dynamic load response were improved by using the proposed good approximate 2DOF digital controller. A control algorithm has been implemented with a short sampling time using DSP. This fact demonstrates the usefulness and practicality of our method. The future work is experimental studies on a sudden change of the input voltage.

REFERENCES

Guo, L., J. Y. Hung, and R. M. Nelms (2003), Digital controller Design for Buck and Boost Converters Using Root Locus, *IEEE IECON'2003*, pp.1864-1869.

Guo, H., Y. Shiroishi and O. Ichinokura (2003), Digital PI Controller for High Frequency Switching DC/DC Converters Based on FPGA,*IEEE INTELEC'03*, pp.536-541.

Higuchi, K., K. Nakano, K. Araki and F. Chino (2002),NEW ROBUST CONTROL OF PWM POWER AMPIFIER, *IFAC 15th Triennial World Congress*, (CD-ROM).

Higuchi, K., K. Nakano, T. Kajikawa, K. Araki and F. Chino (2003).Robust Control of PWM Power Amplifier by Approximate 2-Degree-of-Freedom Digital Controller with Bumpless Mode Switching,*IEEE IECON'2003*, pp.1835-1840.

Fukuda, H. and M. Nakaoka (1993), State-Vector Feedback Controlled-based 100kHz Carrier PWM Power Conditioning Amplifier and Its High-Precision Current-Tracking Scheme, *IEEE IECON'93*, pp.1105-1110.